ELECTRICAL RESISTIVITY SURVEYS OF THE ROTOKAWA GEOTHERMAL FIELD, NEW ZEALAND

G. F. RISK

Institute of Geological and Nuclear Sciences, Lower Hutt

SUMMARY – Electrical resistivity surveys of the Rotokawa geothermal field, using the Schlumberger traversing, Schlumberger soundings and multiple-source bipole-dipole measuring methods show a low resistivity anomaly associated with the field. The resistivity structure within the field was inferred from the soundings and by applying 3-D computer modelling to the bipole-dipole data. The lowest resistivities (ca. 2 Ωm) occur at shallow depths (down to 250-400 m depth) representing the hydrothermal reservoir comprising high temperature thermal fluids in altered silicic pyroclastic rocks. Below this conductive layer, resistivity increases (to c. 20 Ωm) reflecting the denser rhyolites, ignimbrites and andesites encountered by drilling and the presence of resistive clay species. At the edge of the field the observed lateral increase of resistivity, to about 700 m depth, defines a resistivity boundary zone which encloses a conductive region of area about 17-28 km^2.

1. INTRODUCTION

The Rotokawa geothermal field (Fig. 1) is situated in the Taupo Volcanic Zone (TVZ) of New Zealand. It lies in the valley of the Waikato River about 12 km NE of Lake Taupo. Thermal ground occurs from Lake Rotokawa in the south to the slopes of Mt. Oruahineawe in the north.

Early geothermal development at Rotokawa, which was done in stages by N.Z. Government agencies; included drilling of holes RK1, RK2 (1965/66); RK3 (1977); and RK4, RK5, RK6, RK8 (1984/85). The depths of these holes ranged from 820 to 2,500 m and all encountered temperatures above 275 °C, the hottest being 325 °C. Recent developments by privately-owned companies and local landowners include another deep hole (RK9), some shallow holes and the commissioning of a 24 MW Power Station (Cole and Legmann, 1998)

Most of the resistivity data described here were measured as part of the 1984/85 exploration effort to provide a more accurate definition of the resistivity low associated with the Rotokawa field than had been available previously. These data were used as a guide for siting drillholes RK5, RK6 and RK8. This paper presents all the available resistivity data and interprets them in terms of the extent and geological structure of the field.

2. GEOLOGICAL SETTING

Early studies in the TVZ noted thermal activity at Lake Rotokawa, along the banks of the Parariki Stream and on the west face of Mt. Oruahineawe (Grange, 1937). Drillholes reveal a flat-lying sequence of volcanic rocks to c. 2 km depth (Fig. 2; Browne *et al.*, 1992). In the top 1.0 – 1.5 km the sequence comprises pumice, pumiceous breccias, lacustrine sandstones and siltstone, unwelded tuffs, rhyolites and ignimbrites. Thick flows of dense Rotokawa Andesite, down-faulted to the NW, form the deepest volcanic formation which rests directly on greywacke basement in RK4.

Gregg (1958) and Fisher and Dickinson (1960) mapped the Rotokawa thermal features and measured the natural heat output, which is currently assessed at 300 MW (Bibby *et* al., 1995). Aeromagnetic surveys over Rotokawa have been made by Gerard & Lawrie (1955) and Soengkono *et al.*, 1991). Hochstein *et al.* (1990) found a self potential high (+200 mV) over the main region of thermal activity. Gravity surveys by Beck and Robertson (1955) and Hunt and Hanns (1990) were interpreted to infer the distribution of dense volcanic and basement rocks.

3. RESISTIVITY MEASUREMENTS

Success with resistivity surveying for delineating hot water dominated geothermal fields hinges on exploiting the contrast between the low resistivities of the hot, water-saturated, hydrothermally-altered rocks inside the reservoirs and the much higher resistivities of the surrounding cold rocks.

3.1 Resistivity mapping surveys

The first phase of resistivity mapping throughout the TVZ (1963 – 65) used the Wenner electrode array (a=550 m) and included a survey of the Rotokawa region (Hatherton *et* al., 1966). This survey first found that a large region of low resistivities coincided with the thermal ground at Rotokawa but it was not sufficiently detailed to provide an accurate outline of the geothermal field.

The region was resurveyed in the mid-1970s using Schlumberger arrays of two sizes:- AB/2 = 500 m and 1000 m. (AB/2 is the distance from the centre to the outside of the array.) These data, which were published as resistivity contour maps

(Geophysics Division, 1985), show that the resistivity low extends further to the north of the Waikato River than shown in the earlier Wenner array maps.

Since then, additional Schlumberger array resistivity measurements have been made. Figs. 3a and 3b show up-dated resistivity contour maps for AB/2 = 500 m and 1,000 m, respectively. The contours are dotted in several places indicating either poor coverage of measurement sites or conflicting data. In some areas, particularly in the vicinity of Mt. Oruahineawe (location in Fig. 1), coverage of field sites is poor because obstacles prevented the laying-out of the array. The results show a large continuous area of low resistivity (3 – 10 Ωm) that encloses all the thermal ground at Rotokawa and delineates the geothermal reservoir to about 500 m depth.

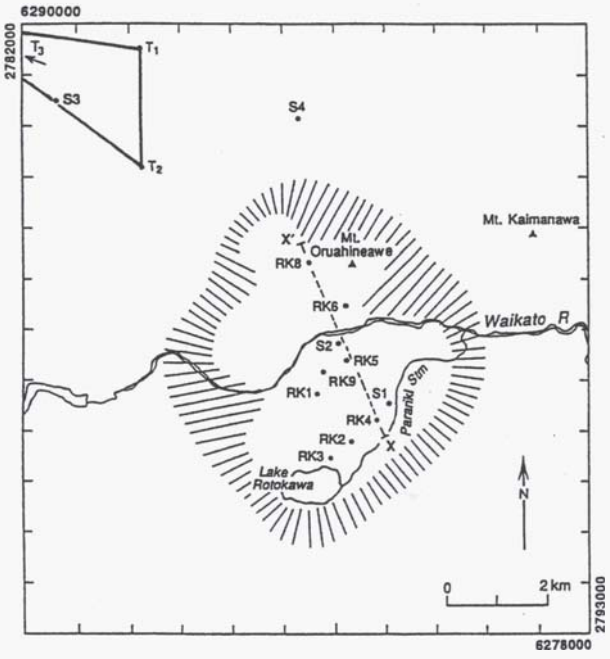

Figure 1: Rotokawa geothermal field showing drillholes (RK1 – RK9), Schlumberger resistivity sounding sites (S1 - S4), Multiple-source bipole-dipole transmitter electrodes (T_1, T_2, and T_3; T_3 lies 1.3 km east of the NE corner of the map). Hatching shows inferred resistivity boundary.

3.2 Schlumberger Resistivity Soundings

Vertical electrical soundings using Schlumberger electrode arrays expanded from AB/2 = 2 m to about AB/2 = 2000 m were made at four sites (S1 – S4, Fig. 1). These data and their interpretations as horizontally-layered models are shown in Fig. 4.

The shapes of the sounding curves from sites inside the field (S1, S2) contrast strongly to those from sites outside the field (S3, S4). At S1 and S2, which are near drillholes RK4 and RK5, surface layers of high-resistivity pumice (>1,000 Ωm) and partly altered volcaniclastics (20–50 Ωm) extend to about 20 – 30 m below the surface. Beneath this lies the low-resistivity layer (1.8 – 3 Ωm; up to 400 m thick) which gives rise to most of the resistivity anomaly associated with the Rotokawa field. Below the main conductive layer resistivity increases with depth, which is discussed below.

In contrast, the sounding curves at sites S3 and S4 show that the high-resistivity (>300 Ωm) surface layers extend to 550 – 800 m depth, and the 3 Ωm layer is absent. Hence, there has been no significant thermal activity at these sites since the deposition of the resistive volcaniclastics. Below about 500 m at all four sites, resistivities cannot be accurately determined but lie in the range 15 – 50 Ωm.

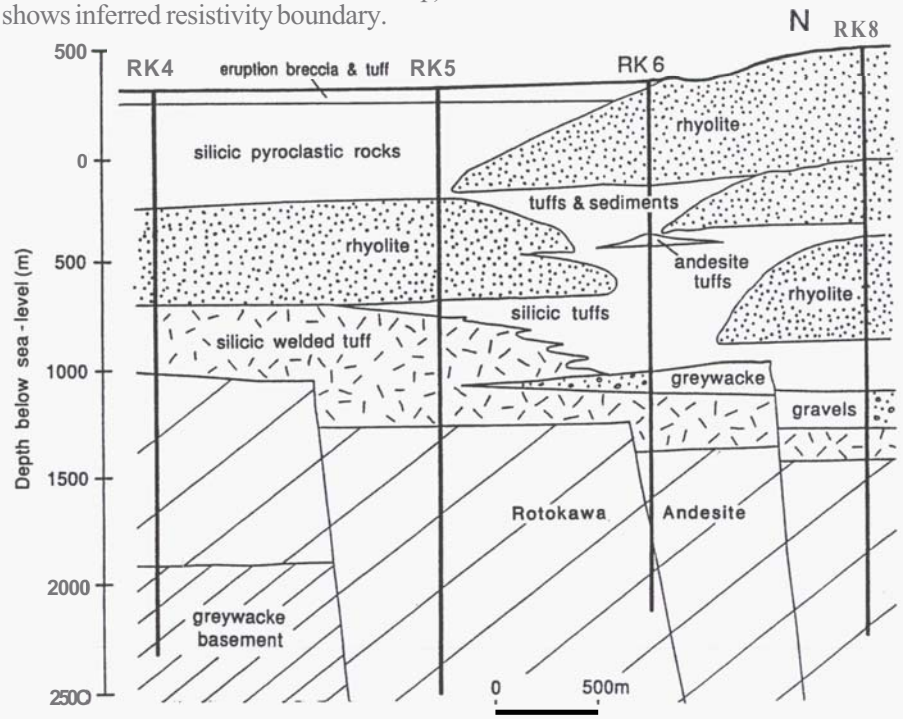

Figure 2. Geological cross-section of Rotokawa field along transect XX′ (Browne et al., 1992).

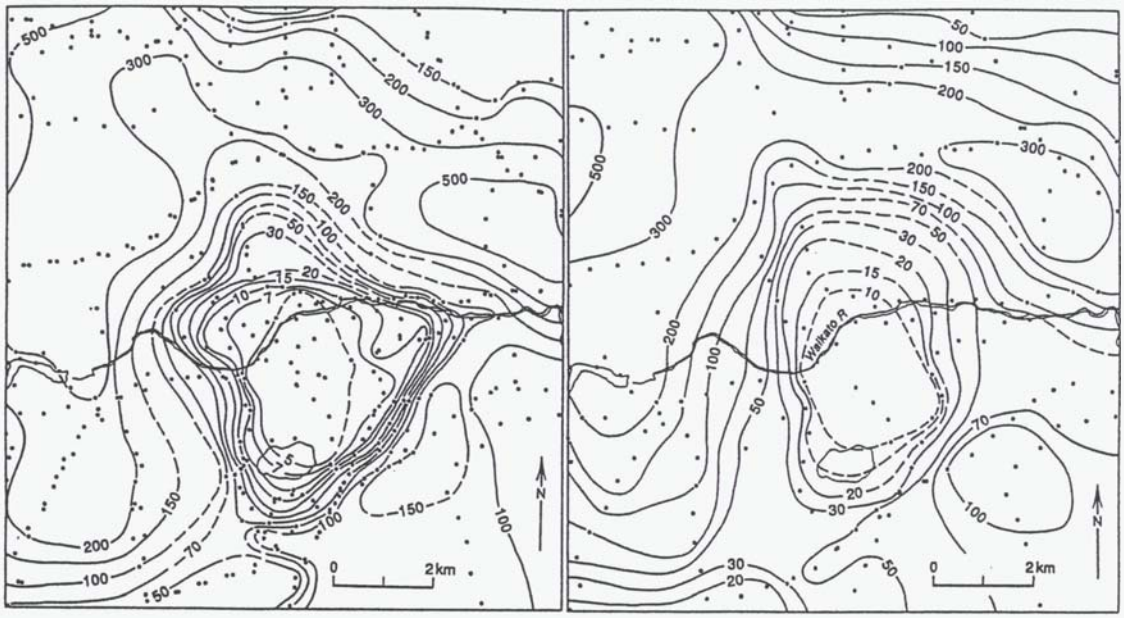

Figure 3. Schlumberger array apparent resistivities in Ωm, (a) AB/2 = 500 m, (b) AB/2 = 1,000 m.

3.3 Multiple-source bipole-dipole survey

In September 1984, a further resistivity survey of the Rotokawa region was made using the multiple-source bipole-dipole method (Risk et *al.*, 1970). For this survey, a transmitter consisting of three current bipoles was operated from a fixed position about 5 km north of the Rotokawa field. The electric fields caused by the flows of current (19 to 26 A) were measured at the field sites using mobile 2-channel receiver units connected to two perpendicularly-oriented grounded dipoles.

3.4 Total field apparent resistivities

From the independent sets of field data that were measured with the three transmitter bipoles (T_1-T_2, T_2-T_3, T_3-T_1, in Fig. 1) the corresponding total field apparent resistivities were calculated using the method described in Risk et *al.* (1970). These are shown in Figs. 5a, 5b and 5c as contour maps. Sharp contrasts in total field apparent resistivity at the edges of the Rotokawa low-resistivity anomaly are obtained only in places where the current crosses the edge of the field nearly perpendicularly. The sharpest contrasts occur across the NW boundary in Figs. 5a and 5b and across the SE boundary in Fig. 5b. Where the current flow strikes nearly parallel to the field boundary the total field apparent resistivities show no sharp change across the boundary. Thus, total field apparent resistivities must be used with caution for delineating the field.

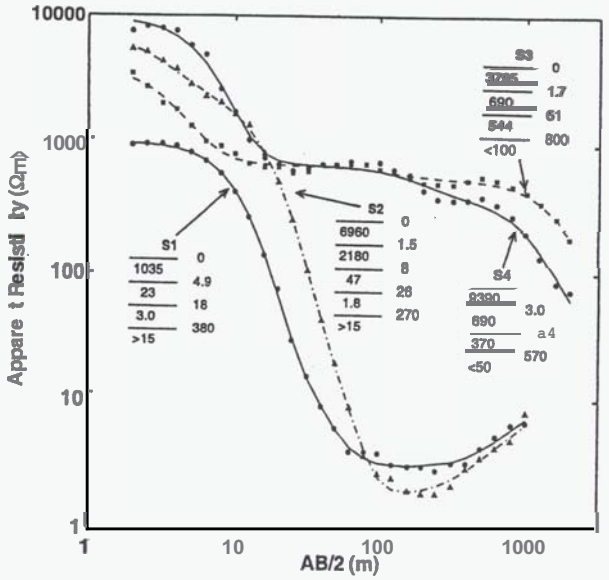

Figure 4. Schlumberger resistivity soundings. Dots show measured data. Curves show calculated resistivities for indicated sections (left column: resistivities in Ωm; right column: depths in metres).

3.5 Apparent Resistivity Tensor Analysis

A more satisfactory way of obtaining apparent resistivities from multiple-source bipole-dipole data is to apply tensor analysis to all three data sets (T_1-T_2, T_2-T_3, T_3-T_1) simultaneously, following the method established by Bibby (1977, 1986). From this process a single apparent resistivity tensor is defined for each field site.

These apparent resistivity tensors can be displayed in various ways. In Fig. 5d they are represented as apparent resistivity ellipses which illustrate how resistivity varies with both azimuth and horizontal position. The low-resistivity region associated with the Rotokawa field shows as a zone with ellipses of small area. Outwards across the boundary of the field, the ellipses change orientation and increase in size, indicating the extent of the low-resistivity anomaly.

The apparent resistivity tensor can also be represented by various scalar tensor invariants that remain unchanged under rotation of the coordinate frame. Fig. 6a displays the measured apparent resistivity invariant P_2, which is an average apparent resistivity proportional to the area of the ellipses in Fig. 5d. In Fig. 6a, the 30 Ωm contour

approximately outlines the, field. Within the field there are several zones where apparent resistivities are noticeably less than average (<20 Ωm) and one where they are greater than average (>20 Ωm). These will be discussed later.

3.6 Computer Modelling

Three dimensional computer modelling of the P_2 apparent resistivity data was done using the computer programs and techniques developed by Hohmann (1975) and Bibby & Hohmann (1993). This modelling involves iteratively adjusting the locations, sizes, and resistivities of cubic blocks in a 3-D array until a match is achieved between the patterns of apparent resistivities obtained from the models and those of the measurements. The smallest cubes measured 0.5 km along a side, which limits the resolution of detectable structures, particularly, the thickness of the shallow layers.

It was found that the modelling process did not lead to a unique solution, but could be improved by applying constraints from knowledge of near-surface resistivities, the resistivity soundings and other information about deep and peripheral parts of the region. Fig. 6c shows cross-sections of the best-fitting model from which the theoretical P_2 apparent resistivities in Fig. 6b were obtained.

While other more complex models are able to generate a slightly'better fit, the model in Fig. 6b contains the essential elements. The principal feature is the low-resistivity layer at 0.2 km depth which in the model has a thickness of 0.5 km (the minimum allowable). This layer is an approximate representation of the low-resistivity layer found in the soundings S1 and S2 (Fig. 4) to be between 240 and 360 m thick. Its resistivity is about 2.5 Ωm in most places, but is smaller (c. 1.0 Ωm) in three

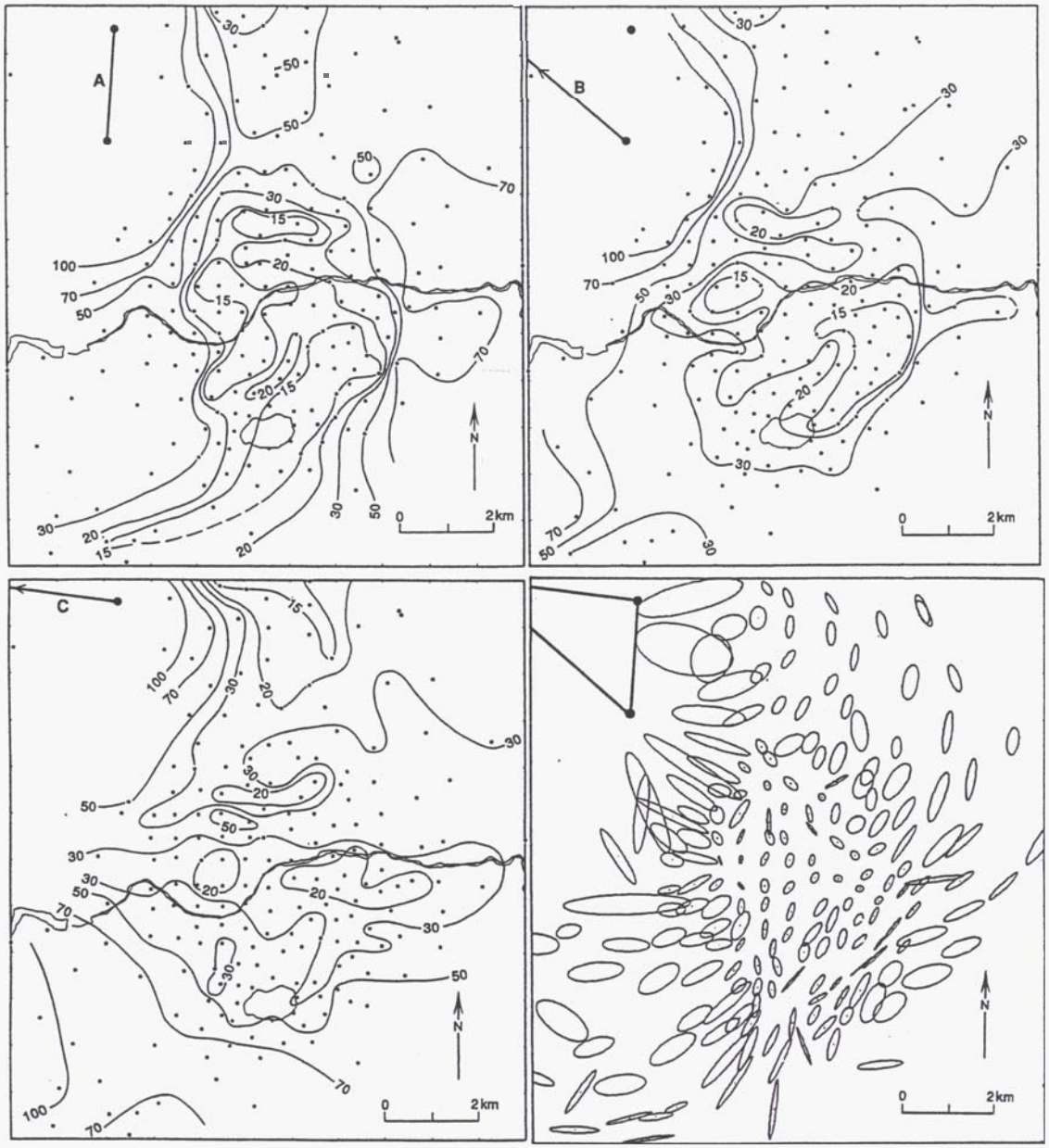

Figure 5. Multiple-sourcebipole-dipole survey using the transmitters shown in NW of the diagrams. (a) Total field apparent resistivities in Ωm for bipole source T_1-T_2; (b) source T_2-T_3 ; (c) source T_3-T_1 . (d) Apparent resistivity tensors represented as ellipses.

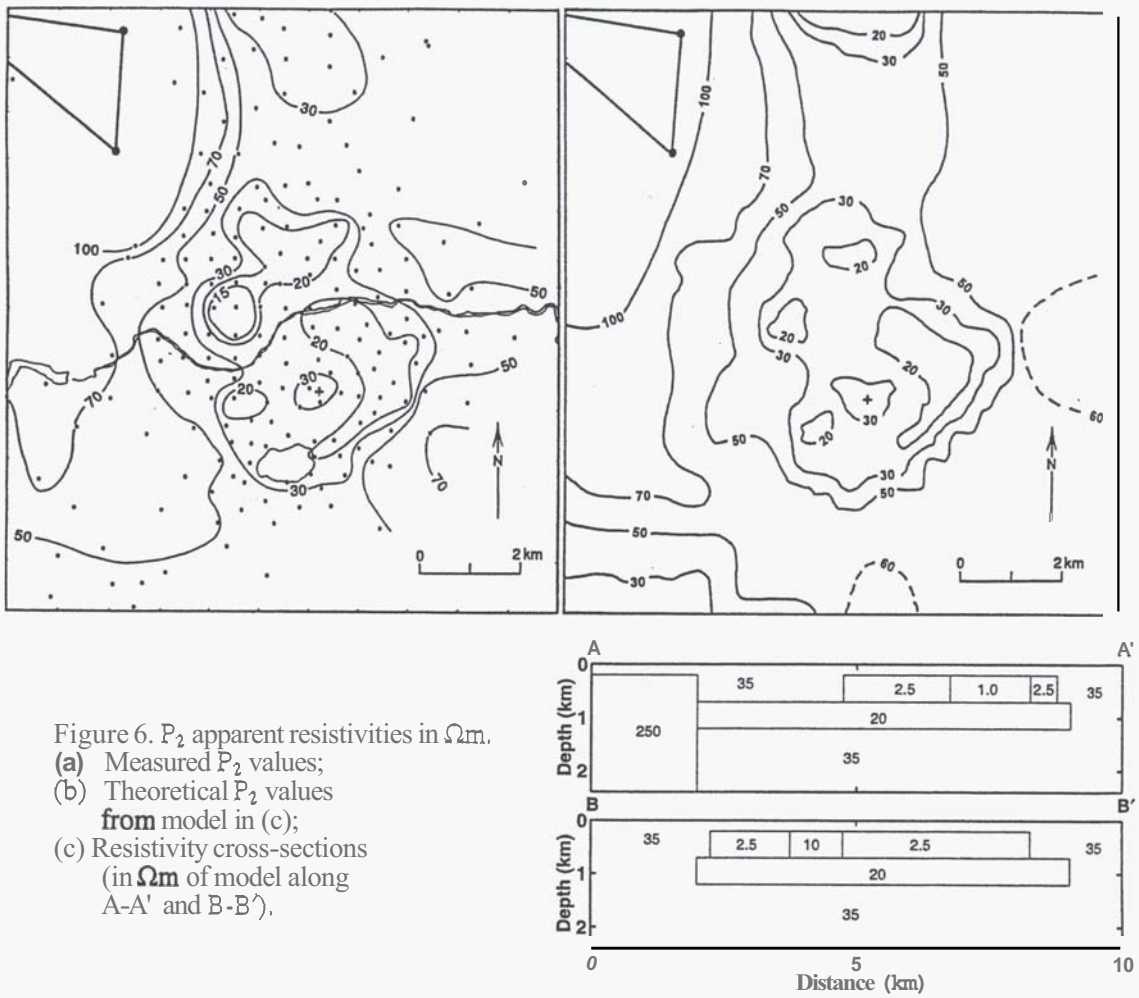

Figure 6. P_2 apparent resistivities in Ωm.
(a) Measured P_2 values;
(b) Theoretical P_2 values from model in (c);
(c) Resistivity cross-sections (in Ωm of model along A-A' and B-B').

zones (which approximately coincide with the lowest P_2 anomalies in Fig. 6a) and is greater (c. 10 Ωm) in a small zone just north of Lake Rotokawa. These resistivity variations in the model may, in the field, represent variations of thickness of the conductive layer, as discussed below.

Below the low-resistivity layer, resistivity increases with depth to 20 Ωm at 0.7 km depth, and to 35 Ωm at 1.2 km. The modelling was insensitive to the resistivity values of layers deeper than about 1.5 km depth and contour maps similar to Fig. 6b could be obtained with the deep resistivity as high as 60 Ωm. Ensuring a good fit requires the model to also contain large high-resistivity blocks to the west of Rotokawa (and beneath the current electrodes), and low resistivity blocks (off map) to represent the neighbouring low-resistivity fields at Ngatamariki, Tauhara and Wairakei.

4. DISCUSSION

Clear differences between the positions and shapes of the resistivity contours on Figs. 3, 5 and 6 confuse the issue of locating of the edge of the low-resistivity structure. The Schlumberger traversing data with AB/2 = 500 m in Fig. 3a give the best definition of the resistivity boundary at c. 100-300 m depth except in places with few measurements, while the tensor resistivity data (Figs. 5d and 6a) are best in the range 500 – 1,000 m. The computer modelling shows that the 30 Ωm contour in Fig. 6b approximately coincides with the outer boundary of the shallow low-resistivity layer in the model.

From the resistivity observations and the modelling the lateral resistivity boundary zone of the Rotokawa field has been constructed as shown in Fig. 1. It is shown as an annular region across which resistivity grades from low on the inside to high on the outside. The width of the zone reflects both the width of the transitional region between hot and cold and the uncertainty of the interpretations after measurement density and errors are taken into account. The inside boundary covers 17 km^2 and the outside boundary 28 km^2.

The modelling shows that the largest block of very low resistivity rock (1 –2 Ωm; <500 m thick) occurs in the SE of the field along the valley of the Parariki Stream and is approximately outlined by the eastern 20 Ωm contour in Fig. 6a. These very low resistivities are consistent with the highly altered nature of the rocks in this zone and the acidity of the near-surface thermal waters, suggesting that this part of the field has been thermally active for a very long time. Two smaller very low resistivity blocks occur in the east of the field.

The zone of higher-than-average shallow resistivity about 2 km north of Lake Rotokawa (Fig. 6a) may represent the presence of a high-resistivity

structure not yet encountered by drilling. Alternatively it may be caused by a thinning of the conductive layer. Such a thinning may indicate an increase in level of the boundary between the conductive smectite-rich clay species and the underlying more resistive illite-rich clays. This phenomenon has been reported by Anderson *et* al. **(1999)** in overseas geothermal fields.

Modelling of aeromagnetic data (Soengkono *et* al., **1991)** reveals the existence of a demagnetised body of rock within the Rotokawa field. The western edge of this body nearly coincides with the western part of the resistivity boundary zone (Fig. **1)** and may mark the edge of a shallow seated rhyolite flow which causes a strong magnetic anomaly centred to the west of Rotokawa.

The high resistivities between Rotokawa and Wairakei indicate that a hydrological connection between the thermal fluids in the two systems is unlikely. But, whether there are connections between Rotokawa and either Tauhara (to the SW) or Ngatamariki (to the N) cannot be readily determined from these data.

The main purpose of this paper is to formally present the map of the resistivity boundary zone of the Rotokawa geothermal field (Fig **1)** along with the resistivity information on which it is based. This resistivity boundary has been available since **1985** and has been used as a guide for siting drillholes, for planning and resource allocation purposes and in scientific papers to illustrate the extent of the field. The results of the bipole-dipole resistivity and the computer modelling have not previously been published.

5. ACKNOWLEDGEMENTS

Assistance with the field measurements from H H Raper, G B Dawson, S L Bennie, D J Graham, V M Stagpoole and T C Mumme is gratefully acknowledged. I am also grateful for helpful comments on the manuscript from H.M. Bibby, V.M. Stagpoole, C.J. Bromley and I.J. Graham. This paper is GNS Contribution No. **2037** and the work has been partially funded by Foundation for Research, Science and Technology Contract C05X0004.

6. REFERENCES

Anderson, E., Crosby, D., Ussher, G. **1999.** As plain as the nose on your face: Geothermal systems revealed by deep resistivity. Proceedings of **21st** New Zealand Geothermal Workshop, **107-112.**

Beck, A.C., Robertson, E.I., **(1955).** Chapter **2:** Geology and Geophysics in Grange. L.I. (comp.) Geothermal steam for power in New Zealand, DSIR Bulletin **117, 15-19.**

Bibby H M, **1977:** The apparent resistivity tensor. Geophysics **42,1258-1261.**

Bibby H M, **1986:** Analysis of multiple-source bipole-dipole resistivity surveys using the apparent resistivity tensor. Geophysics **51,972-983.**

Bibby H M, Hohmann G W, **1993:** Three-dimensional interpretation of multiple-source bipole-dipole data using the apparent resistivity tensor. Geophysical Prospecting, **41,697-723.**

Bibby H M, Caldwell, T.C., Davey, F.J., Webb, T.H. **1995:** Geophysical evidence on the structure of the Taupo Volcanic Zone and its hydrothermal Circulation. Journal Of Volcanological and Geothermal Research, **86, 29–58.**

Browne P R L, Graham I J, Parker R J, Wood C P, **1992:** Subsurface andesite lavas and plutonic rocks in the Rotokawa and Ngatamariki geothermal systems, Taupo Volcanic Zone, New Zealand. J. Volc.& Geoth. Res., **51,** 199-215.

Cole, B., Legmann, H., **1998.** The Rotokawa geothermal project: a high pressure, sustainable and environmentally benign power plant. Geoth. Res. Council Transactions **22,509-513.**

Fisher R G, Dickinson D J, **1960:** The natural heat flow from the Rotokawa area. Geothermal Circular TSG **10, 6** pp. & 1 map.

Gerard V B, Lawrie J A, **1955:** Aeromagnetic surveys in New Zealand **1949-1952.** Geophysical surveys in New Zealand. Geophysical Memoir **3,** DSIR, Wellington. **20** pp. & **6** maps.

Geophysics Division, DSIR, **1985:** Sheet **U17** - Wairakei. Electrical Resistivity map of New Zealand **1:50000.** Nominal Schlumberger array spacings *500* m and 1,000 m. DSIR, Wellington.

Grange L I, **1937:** The Geology of the Rotorua-Taupo subdivision, NZ Geol.Surv.Bull.37, **138** p.

Gregg D R, **1958:** Natural heat flow from the thermal areas of Taupo sheet District **N94. N.Z.** J. Geol. Geophys. **1: 65-76.**

Hatherton T, Macdonald W J P, Thompson G E K, **1966:** Geophysical methods in geothermal prospecting in New Zealand. Bulletin Volcanologique **29: 485-98.**

Hochstein M P, Mayhew I D, Villarosa R A, **1990:** Self-potential surveys of the Mokai and Rotokawa high temperature fields (NZ). Proceedings of 12th New Zealand Geothermal Workshop, **87-90.**

Hohmann G W, **1975:** Three dimensional induced polarization and electromagnetic modelling. Geophysics **40,309-324.**

Hunt T M, Harms C, **1990:** Gravity survey of the Rotokawa geothermal field. Proceedings of 12th New Zealand Geothermal Workshop, **91-96.**

Risk G F, Macdonald W J P, Dawson G B, **1970:** D.C. resistivity surveys of the Broadlands Region, N. Z. Geothermics Special Issue **2(2): 287-94.**

Soengkono S, Hochstein M P, van Dijck M F, **1991:** Magnetic anomalies of the Rotokawa Geothermal Field, Taupo Volcanic Zone, New Zealand. Proc. 13th New Zealand Geothermal Workshop, University of Auckland, **33-38.**